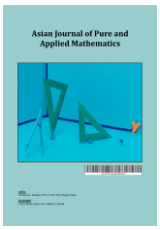

Asian Journal of Pure and Applied Mathematics

Volume 6, Issue 1, Page 59-76, 2024; Article no.AJPAM.1451

Analysis of Bioconvective Steady Darcy Forchhemier Nanofluid Flow with Arrhenius Chemical Kinetics and Energy Transition over a Permeable Vertical Plate

Matilukuro O. M. [a*], Olanrewaju P. O. [a], Amoo S. A. [a] and Nwaokolo M. A. [a]

[a] Department of Mathematics and Statistics, Federal University Wukari, Taraba State, Nigeria.

Authors' contributions

This work was carried out in collaboration among all authors. All authors read and approved the final manuscript.

Article Information

Open Peer Review History:
This journal follows the Advanced Open Peer Review policy. Identity of the Reviewers, Editor(s) and additional Reviewers, peer review comments, different versions of the manuscript, comments of the editors, etc are available here: https://prh.globalpresshub.com/review-history/1451

Original Research Article

Received: 27/10/2023
Accepted: 02/01/2024
Published: 24/01/2024

Abstract

In the realm of renewable energy, Darcy-Forchheimer nanofluids are considered for use in solar collectors and thermal energy storage systems. Magnetohydrodynamics Bioconvective Unsteady Darcy Forchhemier Nanofluid flow with arrhenius chemical kinetics and energy transition over a permeable vertical plate was considered. The Darcy Forchheimer porosity medium was considered for the flow analysis. The impressions of thermal radiation, viscous dissipation, heat generation, activation energy, Soret and Dufour effects are taken to investigate the transference analysis of heat and mass rate. The flow equations are in the form of partial differential equations (PDEs) and we utilize suitable similarity transformations to convert them into ordinary differential equations (ODEs). The thermophysical characteristics of the gyrostatic microorganisms conducting flow with energy transition were analysed numerically using

**Corresponding author: E-mail: motikorede@gmail.com;*

Chebyshev Collocation Method (CCM – Hybrid Numerical method) and analytically, using Galarking Weighted Residual Method (GWRM – Analytical technique) with help of MATHEMATICA software. The findings from this research were analyzed in the form of graphs and tables. The following is a list of some key observations from this parametric research: The chemical reaction thermophoresis and Brownian motion parameter reduces the mass concentration, while large values of activation energy have the opposite effect. The mounting values of Péclet numbers (Pe) and bioconvection Lewis numbers reduce the motile microorganism profile. The results obtained showed a perfect agreement with the existing literature and have further applications in fluid dynamic.

Keywords: Bioconvective; darcy forchhemier; nanofluid; arrhenius chemical kinetics.

Symbols	***:***	***Name***
B_0	*:*	*Applied magnetic feld;*
(u, v)	*:*	*Velocity component;*
Q_0	*:*	*Heat generation/absorption;*
$k = k_0 x$	*:*	*Initial permeability;*
g	*:*	*Gravity;*
σ	*:*	*Electrical conductivity;*
$f_w < 0$	*:*	*Injection;*
Wc	*:*	*Cell moving speed;*
N	*:*	*Concentration of the microorganisms;*
n_w	*:*	*Density of motile microbes;*
T_w	*:*	*Surface temperature;*
$f_w = 0$	*:*	*Surface impermeability;*
Gr	*:*	*Grashof number;*
Pe	*:*	*Péclet number;*
Lb	*:*	*Bioconvection Lewis number;*
Ha	*:*	*Hartmann number;*
Nb	*:*	*Brownian motion;*
λ	*:*	*Ratio of the heat capacitance to the base fluid;*

D_B	:	*Brownian diffusion;*
α	:	*Thermal diffusivity;*
D_m	:	*Microorganism's diffusivity;*
β	:	*Volume expansion;*
μ	:	*Viscosity;*
γ	:	*Microorganism average volume;*
ρ_m	:	*Density of microorganisms;*
C_w	:	*Volume fraction of nanoparticle;*
$a > 0$	:	*Stretching rate;*
$f_w > 0$	:	*Suction;*
Rb	:	*Rayleigh number;*
Ec	:	*Eckert number;*
Le	:	*Lewis number;*
Nt	:	*Thermophoresis constraint;*
Nr	:	*Buoyancy ratio;*
Ω	:	*Microorganisms' concentration difference;*
ρ_f	:	*Density;*
B	:	*Chemotaxis coefficient;*
$U_w(x) = ax$	:	*Stretching sheet.*

1 Introduction

The quest to increase thermal conductivity of liquid, was primarily observed and shown to have experimentally produced what is known today as Nanofluid. [1-2] attributed the birth of nanofluid to revolutionary idea of adding solid particles into base fluid, with the specific aim of increase the thermal conductivity and that a new class of solid/liquid suspensions, offer scientific challenges because their measured thermal conductivity is one order of magnitude greater than predictions. Yu [2] pointed out that "it has long been known that liquid molecules close to a solid surface form layered solid-like structures, but little is known about the connection between this nanolayer and the thermal properties of the suspensions". To this end Yu [3] decided to modify Maxwell [1] equation for "the effective thermal conductivity of solid/liquid suspensions to include the effect of this ordered nanolayer. Because this ordered nanolayer has a

major impact on nanofluid thermal conductivity when the particle diameter is less than 10 nm, a new direction is indicated for development of next-generation coolants".

Sreelakshmy et al. [4] in their work "overview of recent nanofluid research" corroborated the claim of Maxwell [1] that "Nanofluid have great thermo-physical properties such as thermal conductivity, thermal diffusivity, viscosity and heat transfer coefficient, as compared to their base fluid. Concluding that the key feature of nanofluid is its superior thermal conductivity".

Maatoug et al. [5] "The fact that non-Newtonian fluids have been used widely in industrial and engineering processes over the past few decades has led to an increase in interest among researchers in studying the various models of these fluids. Drilling, plastic polymer, paint, coating sheets, and numerous other procedures are among them". The constitutive equations of the nonNewtonian fluids are higher order, more complex, and nonlinear than those of the Newtonian fluid. "There are three primary types of non-Newtonian fluids: integral, rate, and differential. The Darcy-Forchheimier nanofluid's flow behavior, which was linked to the relationship between shear stress and strain, indicated that the fluid ought to be categorized as a non-Newtonian fluid. High stress rate against dominant shear viscosity is the defining feature of this flow. Although the fluid behaves like a solid when applied tension less than the yield stress, the fluid fluctuates when shear force is applied" Gaffar et al. [6]. "The Darcy-Forchheimier material is a straightforward linear representation in which time derivatives stand in for the more traditional convective products. The relaxation and retardation times parameters are used in the polymer industry to define the viscoelastic characteristics of the polymer itself" Ali and Asghar [7]. "In addition, blood flow through very narrow arteries is characterized as a Darcy-Forchheimier nanofluid due to its rheological properties" Sharma et al. [8]. When it comes to the petroleum industry, convection liquid gush displays in a porous area are crucial for determining the possibility of higher flow rates occurring near wellbores for gas and condensate waterholes. This is due to the likelihood that high flow rates will emerge in these areas. Many modern applications that make use of porous areas can find themselves operating at high velocities. The non-Darcian permeable area is a modified form of Darcy's law that takes into account the effects of both inertia and porous space. The conventional Darcy's equation has been used to model and analyze flow problems across permeable regions in the majority of research on this subject. Nevertheless, at higher velocities and larger porosities, Darcy's theory in its classical form fails Seddeek [9]. The bio-convection pattern is based on the impulsive transport of macroscopic fluids and observed as another devoted research area in bio-engineering and biotechnology. The pattern of bioconvection is accessed as multifaceted interaction of microorganisms at various physical scales. The locomotion of self-objected microorganisms induced the bioconvection pattern. The microorganism pattern is considered as meso-scale phenomenon. The motion of nanoparticles is free of microorganisms swimming and thus, the interaction between Nano-materials and bioconvection leads to the more fascinating micro fluidic applications. The activation energy terminology, which states as the nominal supply of energy acquired to induct a chemical reaction," was established by a Swedish scientist 'Svante Arrhenius' in 1889. Several procedures that include transferal of mass with activation energy are oil container engineering, food production, synthetical processing, oil coating, etc. There are dynamic devices through which chemical reactants are implicated for activating reactions to produce a vast output. [10-12] scrutinized "the influence of activation energy on time-dependent magneto Williamson nanofluid flow. The flow rate could be related to the imposed heat through a linear proportionality involving a constant, k, where "k is a coefficient dependent on the permeability of the (sand) layer."The Arrhenius equation is $K = A\exp\left(-\frac{E_a}{kT}\right)$ where A is the frequency or pre-exponential factor and $\exp\left(-\frac{E_a}{kT}\right)$ represents the fraction of collisions that have enough energy to overcome the activation barrier (i.e., have energy greater than or equal to the activation energy E_a) at temperature *(T)*. Arrhenius in 1889 argued that for reactants to transform into products, they must first acquire a minimum amount of energy, called the activation energy Ea. At an absolute temperature T, the fraction of molecules that have a kinetic energy greater than Ea can be calculated from statistical mechanics. The concept of activation energy explains the exponential nature of the relationship, and in one way or another, it is present in all kinetic theories. Heat conduction through nanoparticles is enhanced because of their small size and large surface area. Nanofluid can be made in two

primary ways". Kazi and Togun, [13] the first is the introduction of synthesized nanoparticles into a host fluid by means such as evaporation or inert-gas condensation. The second strategy includes releasing nanoparticles into the environment.

[14-15] reported "order of magnitude increasing in the critical heat flux in a pool boiling, by comparing Nanofluid to base fluids. The tendency of raising chip power in electronic components or simplifying cooling requirements for space applications is being presented. High critical heat fluxes which allows for boiling to higher qualities with increased heat removal and wider safety margin from film boiling makes Nano fluids attractive in general electronic cooling as well as space applications with very high power density". Sabet [16] Nanofluids can be considered for use in microthrusters and propulsion systems for small satellites and spacecraft. The unique fluidic properties contribute to efficient thrust generation and precise control in microgravity environments. Nanofluids can play a role in improving the efficiency of thermal control systems for life support equipment on spacecraft. This includes regulating temperatures for crewed missions, ensuring the comfort and safety of astronauts.

Farooq et al. [17] investigated "3D flow of magnetized hybrid nanofluid with heat source/sink over a stretching sheet and the results shows that when the angle of inclination, magnetic parameter, and the volumetric concentration of hybrid nonmaterial's increase the axial flow profile of the hybrid nanofluids is reduced". Sharma and Gandhi [18] discussed "the combined effects of Joule heating and non-uniform heat source/sink on unsteady MHD mixed convective flow over avertical stretching surface embedded in a Darcy-Forchheimier porous medium". Gautam et al. [19] examined "comparative study of two non-Newtonian fluids with bioconvective induced MHD flow in presence of multiple slips, heat source/sink and nonlinearthermal radiation and the results shows that the magnitude of surface drag and surface cooling rate are at a higher level for Casson fluid in comparison with Maxwell fluid". Jawad et al. [20] studied "the influence of bioconvection and thermal radiation on MHD Williamson Nano Casson fluid flow with the swimming of Gyrotactic microorganisms due to porous stretching sheet and it was established that through rising the value of bio-convection and Peclet number, the microorganism field diminishing". Asogwaet et al. [21] investigated "the suction effect on the dynamics of EMHD casson nanofluid over an induced stagnation point flow of stretchable electromagnetic plate with radiation and chemical reaction which resulted into an increment in the modified Hartmann number increases the rate of energy, mass flux and friction. As lewis number, Brownian motion, and chemical reaction rise, the thickness of the concentration boundary layer decreases on the stretching Riga surface". Eswaramoorthhi et al. [22] investigated "the exploration of Darcy-Forchheimer flows of non-Newtonian casson and Williamson conveying tiny particles experiencing binary chemical reaction and thermal radiation: comparative analysis". Jawad et al. [23] studied "the influence of Bioconvection and thermal radiation on MHD Williamson Nano Casson fluid flow with the swimming of Gyrotactic microorganisms due to porous stretching sheet which shows the rising the value of bio-convection and Peclet number, the microorganism field diminishing". Nadab et al. [24] investigate "Heat and mass transfer analysis of magnetohydrodynamic (MHD) thermosolutal nanofluid flow over vertical and inclined porous media. The conventional base fluid used in industrial cooling systems often falls short in meeting the requirements of industrial processes". "To address this limitation, a modern phase of nanotechnology has been proposed to enhance the cooling rate in industrial processes. Nanofluids offer potential applications in various areas, including car cooling systems, shock absorbers, and the improvement of refrigeration and air-conditioning systems" Yusuf et al. [25]. Abdelmalek et al. [26-29] examined "gyrotactic bacteria's one-of-a-kind characteristics in Williamson nanofluid's incompressible flow by looking at their second-order slip characteristics and activation energy".

2 Mathematical Formulation

The boundary layer gyrostatic microorganisms conducting flow water-based nanoliquid across a vertical permeable plate is addressed in the present work. A constant transversal magnetic field of intensity B_0 is applied to the flow. The Hall effects and magnetic field are inconsequential since there is no magnetic Reynolds number and voltage is modest. As stated, the presence of nanoparticles is expected to not influence

the velocity and direction of microorganisms' movement. The nanoparticulate dispersion is considered to be steady (no nanoparticle coagulation) and dilute (no particulate concentration more than 1%). This is a reasonable postulation because nanoliquid bioconvection is only predicted to occur in a diluted suspension of nanomaterials; otherwise, a high concentration of nanomaterials would raise the base fluid's viscosity, suppressing bioconvection. The framework for bioconvection due to oxytactic microbes is premised on the methodology Algehyne et al. [30].

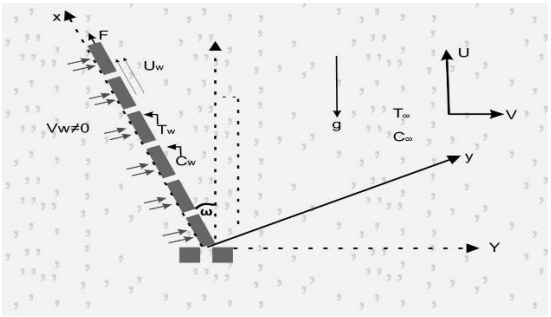

$$\frac{\partial u}{\partial x}+\frac{\partial v}{\partial y}=0 \tag{1}$$

$$u\frac{\partial u}{\partial x}+v\frac{\partial u}{\partial y}=-\frac{1}{\rho}\frac{\partial \rho}{\partial x}+r\frac{\partial^2 u}{\partial y^2}-\frac{\sigma {B_0}^2 u}{\rho}+\frac{1}{\rho}\left[\begin{matrix}(1-\phi_m)\rho(T-T_\infty)\beta_g-(\rho_p-\rho)\\(C-C_\infty)g-(n-n_\infty)(\rho_m-\rho)g_\gamma\end{matrix}\right]$$
$$-\frac{\upsilon}{k}(u-u_\infty)-\frac{k'}{\sqrt{k}}\left(u^2-{u_\infty}^2\right) \tag{2}$$

$$u\frac{\partial T}{\partial x}+v\frac{\partial T}{\partial y}=\alpha\left(\frac{\partial^2 T}{\partial x^2}+\frac{\partial^2 T}{\partial y^2}\right)+\lambda\left[D_b\frac{\partial C}{\partial y}\frac{\partial T}{\partial y}+\left(\frac{D_T}{T_\infty}\right)\left(\left(\frac{\partial T}{\partial x}\right)^2+\left(\frac{\partial T}{\partial y}\right)^2\right)\right]+\frac{\mu\alpha}{k}\left(\frac{\partial u}{\partial y}\right)^2$$
$$+\alpha\frac{\sigma B_0^2}{k}\mu^2+\frac{Q_0}{(\rho c)_f}(T-T_\infty)-\frac{1}{(\rho c)_f}\frac{\partial q_r}{\partial y}+\frac{D_m k_r}{c_s c_p}\frac{\partial^2 C}{\partial y^2} \tag{3}$$

$$u\frac{\partial C}{\partial x}+v\frac{\partial C}{\partial y}=D_B\left(\frac{\partial^2 C}{\partial x^2}+\frac{\partial^2 C}{\partial y^2}\right)+\left(\frac{D_T}{T_\infty}\right)\left(\frac{\partial^2 T}{\partial x^2}+\frac{\partial^2 T}{\partial y^2}\right)-k_r(C-C_\infty) \tag{4}$$

$$u\frac{\partial n}{\partial x}+v\frac{\partial n}{\partial y}+\frac{bW_c}{C_w-C_\infty}\left(\frac{\partial}{\partial y}\left(n\frac{\partial c}{\partial y}\right)+\frac{\partial}{\partial x}\left(n\frac{\partial c}{\partial x}\right)\right)=D_m\left(\frac{\partial^2 n}{\partial x^2}+\frac{\partial^2 n}{\partial y^2}+2\frac{\partial^2 n}{\partial y\partial x}\right) \tag{5}$$

The corresponding boundary conditions are given by

$$\left.\begin{matrix}u=U_\infty(x),\ v=V,\ \ T=T_w,\ C=C_w\ \ n=n_w\ at\ \ y=0\\u=0,\ v=0,\ \ T\to T_\infty,\ \ C\to C_\infty\ ,\ n\to n_\infty\quad\ as\ \ y\to\infty\end{matrix}\right\} \tag{6}$$

With the following similarities variables

$$\eta=y\sqrt{\frac{a}{\upsilon}},\ \psi=\sqrt{a\upsilon}xf\ \ ,\ u=\frac{\partial\psi}{\partial y},\ \ v=-\frac{\partial\psi}{\partial x}\ ,\ \theta=\frac{T-T_\infty}{T_w-T_\infty},\ \phi=\frac{C-C_\infty}{C_w-C_\infty},\ X=\frac{n-n_\infty}{n_w-n_\infty}$$
$$T=\theta(T_w-T_\infty)+T_m,\ C=\phi(C_w-C_\infty)+C_\infty \tag{7}$$

Introducing the transformation (7) into (2) to (5).we obtain the simplified form as

$$f'''+ff''-(k_2+1)(f')^2+Gr(\theta-Nr\phi-R_b\chi)-Haf'-k_1f'=0 \quad (8)$$

$$\theta''+Nb\,\mathrm{Pr}\,\theta''+(\mathrm{Pr}+Nb\phi')\theta'+Nt(\theta')^2+Ec\,\mathrm{Pr}\left((f'')^2+Ha(f'')^2\right)+Q\theta+D_k\phi''=0 \quad (9)$$

$$\phi''+lef\phi'+\frac{Nt}{Nb}\theta''-le\lambda\phi=0 \quad (10)$$

$$\chi''+Lbf\chi'-pe(\phi''(\chi+\Omega)+\chi'\phi')=0 \quad (11)$$

Satisfying the conditions

$$\begin{aligned} &f'(0)=1,\quad f(0)=f_w,\quad \phi(0)=1,\quad \theta(0)=1,\quad X_1(0)=1\\ &f'(\infty)=0,\ \phi(\infty)=0,\quad \theta(\infty)=0,\quad X_1(\infty)=1 \end{aligned} \quad (12)$$

$$Lb=\frac{\upsilon}{D_m},\ pe=\frac{bW_c}{D_m},\Omega=\frac{n_\infty}{(n_w-n_\infty)},le=\frac{\upsilon}{D_B},,\ \lambda_1=\frac{k_r^{\,2}}{a},$$

$$N=\frac{16\sigma^*T_\infty^3}{(\rho c_p)3K^*},\ \mathrm{Pr}=\frac{(\rho c_p)\upsilon}{k},Nb=\frac{\lambda D_T(C_w-C_\infty)}{\alpha},Nt=\frac{\lambda D_T(T_w-T_\infty)}{\alpha T_\infty},Ec=\frac{a^2x^2}{(\rho c_p)(T_w-T_\infty)}$$

$$Ha=\frac{\sigma B_0^2}{\rho a},\quad Q=\frac{Q_0\upsilon}{ka},\quad D_k=\frac{D_mk_r(C_w-C_\infty)}{c_pk(T_w-T_\infty)}k_2=\frac{k'(U_w-U_\infty)^2}{a^2x\sqrt{k}},\ Gr=\frac{\beta(1-\phi_m)(T_w-T_\infty)\rho}{\rho a^2x},$$

$$Nr=\frac{(\rho_p-\rho)(C_w-C_\infty)\phi}{\beta_g(1-\phi_m)(T_w-T_\infty)\rho},k_1=\frac{\upsilon(U_w-U_\infty)}{ka^2x}$$

Le = lewis number, Nb = Thermophoresis parameter, Nt = Brownian motion parameter, λ_1 = chemical reaction term, δ_w = relative temperature, E = Activation energy Pr = Prandtl number, Q = heat generation, Ha = Hartman number, Ec = Eckert number, Dk = Dufour Gr = Grashof number, Rb = Rayleigh number, Nr = Radiation parameter. Other physical quantities of interest in this problem, namely; the skin friction parameter $-f''(0)$ and the Nusselt number $-\theta'(0)$ and Sherwood number $-\phi'(0)$ can be easily computed.

3 Numerical Procedures

The set of non-linear ordinary differential equations (8)–(11) with boundary conditions in equation (10) by using symbolic MATHEMATICA software, the ordinary differential equations have been numerically solved with $Pe, \lambda_1, Q, Nt, Ha, Rb, Gr, Lb, k_2$ as prescribed parameters. A step size of $\Delta\eta = 0.001$ was selected to be satisfactory for a convergence criterion of 10^{-7} in nearly all cases. The value of was found to each iteration loop by the assignment statement $\eta_\infty = \eta_\infty + \Delta\eta$. The maximum value of η_∞, to each group of parameters $Pe, \lambda_1, Q, Nt, Ha, Rb, Gr, Lb, k_2$ is determined when the values of unknown boundary conditions at $\eta = 0$ not change to successful loop with error less than 10^{-9}. The thermophysical characteristics of gyrostatic microorganisms conducting flow with energy transition were analysis numerically using Chebyshev polynomial method with the help of MATHEMATICA

software. The accuracy of the technique was established by comparing the values of Nusselt numbers $\left(Nu_x\right)$ with previous published findings. A satisfactory agreement was discovered (see Table 1). In order to guarantee the accuracy of the technique that is currently being used, the values of energy flux $\left(Nu_x\right)$ and mass flux $\left(Sh_x\right)$ for various $\lambda_1 = (0.1, 0.3, 0.5), Q = (1.5, 2.0, 2.5)$ $Nt = (0.1, 3.0, 5.0)$ Ha = (0.5, 0.7, 1.0) show that the finding demonstrate a good agreement (Table 2).

Table 1. Comparison of Nusselt numbers Nu_x for different values of Pr

Pr	Current Study	Makinde and Aziz [31]	Khan and Pop[32]	Abolbashari et al. [33]
0.20	0.1691	0.1691	0.1691	0.1691
0.70	0.4539	0.4539	0.4539	0.4539
2.00	0.9114	0.9114	0.9114	0.9114

Table 2. Values of energy flux Nu_x , and mass flux Sh_x for various parameters

Parameters	Values	GWRM	CCM	GWRM	CCM
λ_1	0.1	2.40842	2.40843	2.594119411	2.594139413
	0.3	2.50343	2.50344	2.68932	2.68934
	0.5	2.60039	2.60039	2.73424	2.73426
Q	1.5	2.13170	2.13168	2.33205	2.33203
	2.0	2.23121	2.23120	2.53812	2.53810
	2.5	2.33774	2.33772	2.73689	
Nt	0.1	2.53787	2.53788	2.65890	2.65891
	3.0	2.40732	2.40733	2.77302	2.77303
	5.0	2.38685	2.38686	2.87134	2.87135
Ha	0.5	2.63422	2.63423	2.72300	2.72301
	0.7	2.72421	2.72422	2.82172	2.82173
	1.0	2.87200	2.87202	2.97551	2.97552

4 Results and Discussion

In order to get a clear insight of the physical problem, the velocity, temperature and concentration have been discussed by assigning numerical values to the parameters encountered in the problem.

Figs. 1 and 2 illustrates the Thermophoresis parameter Nt and Brownian motion parameter Nb on the concentration profile. The Nt and Nb are two crucial processes in the flow of Nanofluid. However, both figures Nt and Nb enhance the concentration profile. As the ambient state continues to be at a greater concentration level, the explanation that could be given to the enhancement of the concentration via Brownian diffusion is Therefore, with the influence of Nb, the mass concentration flows from ambient layers to the solutal boundary layer, increasing the concentration level. On the other hand, in the case of Thermophoresis parameter, the upsurge in temperature can cause the mass to diffuse, which results in a high level of nanoparticles profile. Therefore, it is necessary that the surface temperature and concentration be regulated appropriately with the ambient temperature and concentration in order to get the outcome that is expected. Fig. 3 illustrates the effect of the chemical reaction parameter $\left(\lambda_1\right)$ on mass concentration and shows that different species reacting with one another is a component in the enhancement of the concentration profile. Before a chemical reaction can take place, there is a certain amount of energy that must first be overcome. In addition, this energy is referred to as the activation energy. The molecules

involved in a chemical reaction must have energies larger than the activation energy for the reaction to proceed. Therefore, the mass concentration improves as the value of the activation energy parameter (E) increases (see Fig. 4).

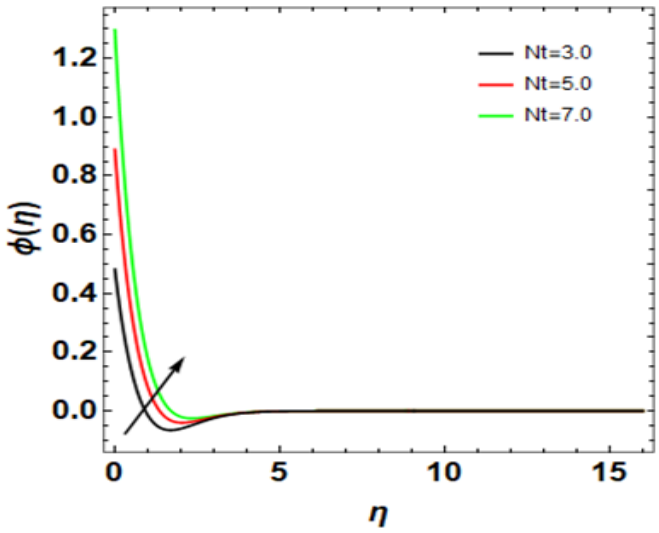

Fig. 1. Effect of thermophoresis *(Nt)* parameter on concentration distribution

Fig. 5 demonstrates that the fluid velocity decreases as the Hartmann number increases. As the Hartmann number Ha increases, a magnetic effect occurs in which a Lorentz force is generated by the magnetic force, and this resistant force works against the motion of the fluid. This reveals that the transverse magnetic field operates in opposition to the transport processes. This occurs since there is more resistance to the transport mechanisms as a result of the Lorentz force, and the response is caused by the magnetic effect. The term "transverse" refers to the relationship between electromagnetic and viscous forces in the field of transport mechanisms. Therefore, the drag force contributes extra resistance to transport processes as a direct result of the reduction in velocity distribution. The Hartmann number is shown to increase the thickness of the thermal boundary layer, as seen in Fig. 6. The influence of magnetic field strength on the temperature profile can be described as the presence of an extra heat source within the channel based on the phenomenon known as Lorentz heating. The increasing value of the Hartmann number causes an increase in the rate at which the fluid temperature is increased in the flow domain. The relationship between thermophoresis and Brownian motion is explained by the governing equations as the result of temperature diffusion along the nanoparticles concentration profile. As a result, there is interaction between the two processes. The Brownian motion occurs as a result of the random motion of the components that make up the system. Therefore, the thermophoresis reduces the temperature distribution, as displayed in Fig. 7. The effect of the heat absorption/generation parameter (Q) is exhibited in Fig. 8. The temperature of the fluid increases as a result of an increase in Q, and an improvement in heat transfer is produced by the heat source. An increase in heat production causes a rise in the temperature as well as an improvement in the thickness of the boundary. The impact of radiation parameter on fluid temperature is display in Fig. 9. The thermal distribution improves with increasing value of thermal radiation. However, these findings may be described by considering the fact that a reduction in the Roseland radiation absorptivity $(k*)$ occurs whenever there is an increase in the Rosseland radiation parameter $q_r = -\dfrac{4\sigma^{*}\partial T^{3}}{KK^{*}}$, for a fixed value of both $(k*)$And (T_{∞}). As $(k*)$ reduces, the radiative heat flux divergence (qr) rises. Hence, the fluid experiences a decrease in the rate of radiative heat transfer. Fig. 10 revealed that the Eckert number (Ec) has a substantial impact on the temperature distribution. This showed the physical situation in which additional thermal energy is provided as the Ec increases to improve the temperature distribution. Therefore, an enhancement in Ec means that the

sheet rate is significantly enhanced, and an increment in fluid motion is also near the sheet. Both of these results are due to the fact that Ec is boosted. The temperature of the fluid increases, particularly in the area close to the sheet. This is because there is a stronger conversion of kinetic energy into heat energy in the boundary layer, which results in an additional viscous heating effect. Hence, there is an enhancement in the boundary layer thickness. The effects of porosity parameter (k_1) and inertial constraint (k_2) on velocity profile are shown in Figs. 11 and 12. Additionally, it is showed that an increase (k_1) and (k_2) slow down the fluid velocity. Bioconvection Rayleigh and buoyancy ratio factors' effects on the dimensionless velocity are depicted in Figs. 13 and 14. With larger values for the bioconvection Rayleigh and buoyancy ratio parameters, the velocity decreases while the Grashof number has opposite behavior is display on the velocity profile.

The effects of Péclet numbers *(Pe)* and bioconvection Lewis numbers *(Lb)* are shown in Figs. 15 and 16. From both figures, the motile microorganism profile decreases with increasing values of Péclet numbers *(Pe)* and bioconvection Lewis numbers *(Lb)*.

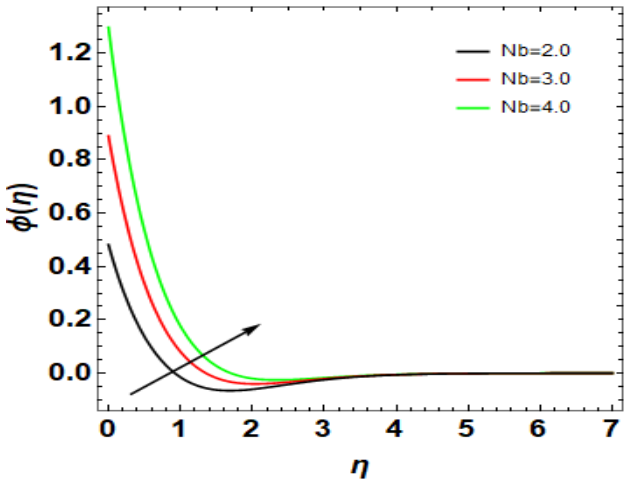

Fig. 2. Effect of brownian motion *(Nb)* on concentration distribution

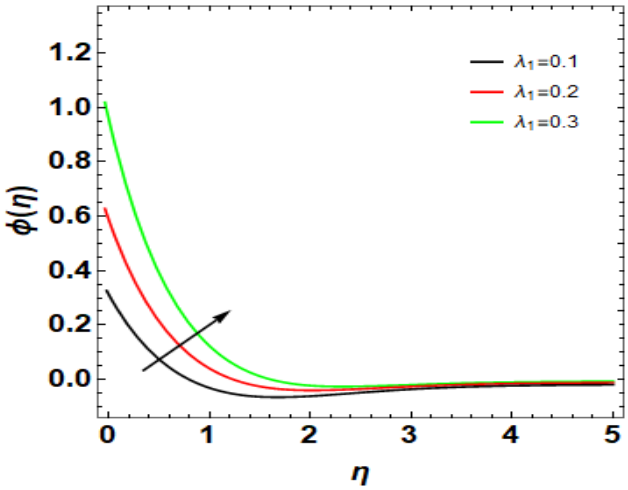

Fig. 3. Effect of reaction constant (λ_1) on concentration distribution

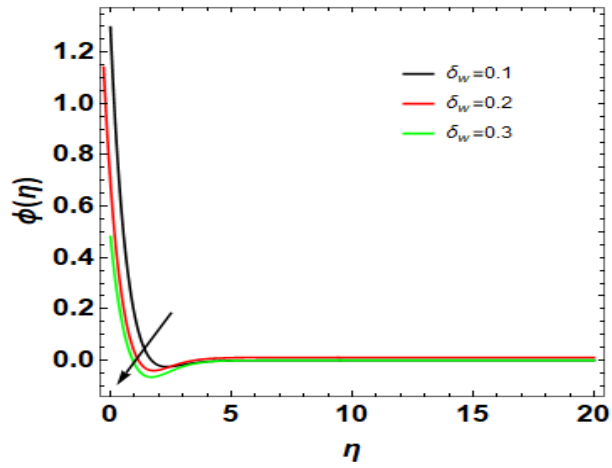

Fig. 4. Effect of activation energy *(E)* on concentration distribution

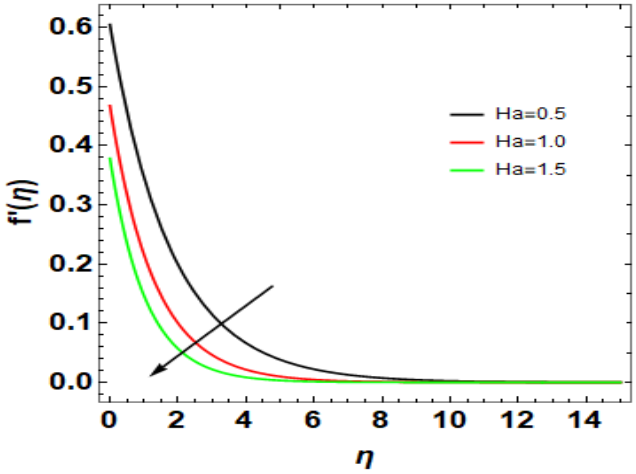

Fig. 5. Effect of Hartman number *(Ha)* on velocity distribution

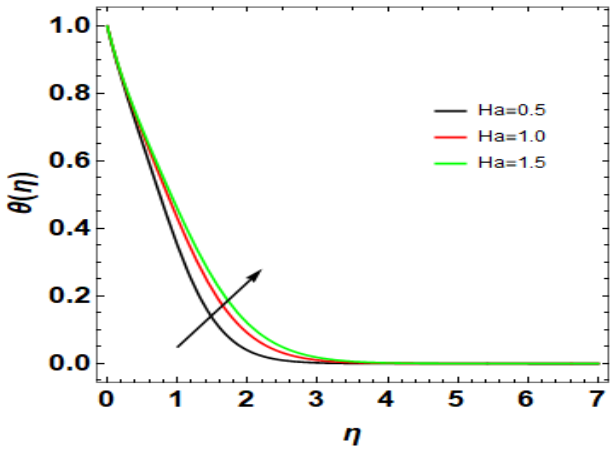

Fig. 6. Effect of Hartman number *(Ha)* on temperature distribution

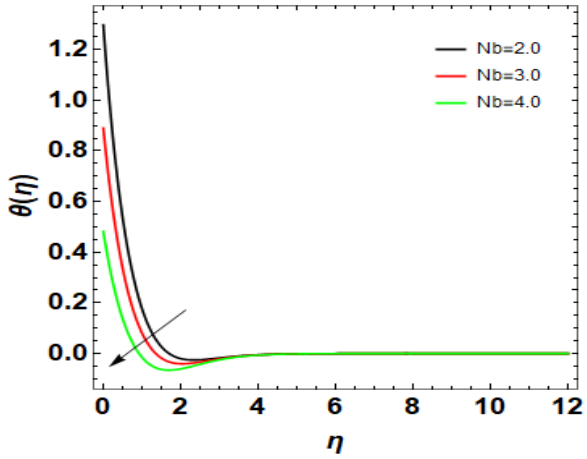

Fig. 7. Effect of Brownian motion *(Nb)* on temperature distribution

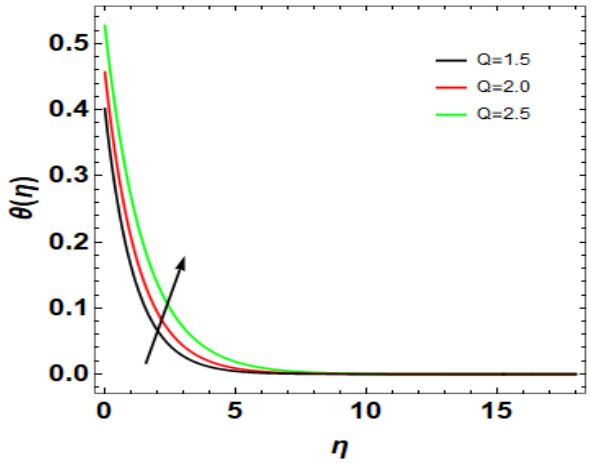

Fig. 8. Effect of Heat and Energy constant *(Q)* on temperature distribution

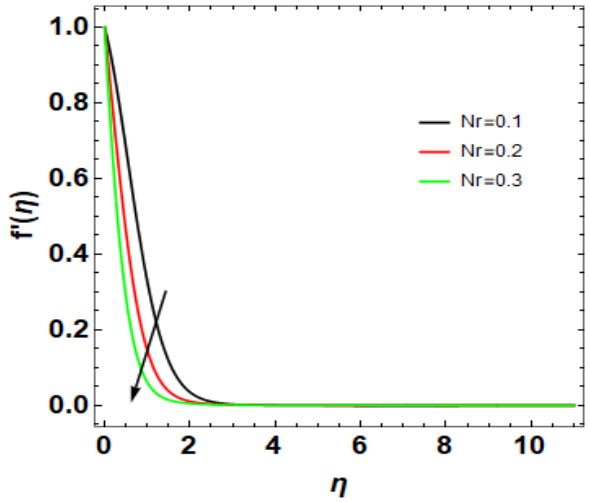

Fig. 9. Effect of Buoyancy ratio (N_r)on velocity distribution

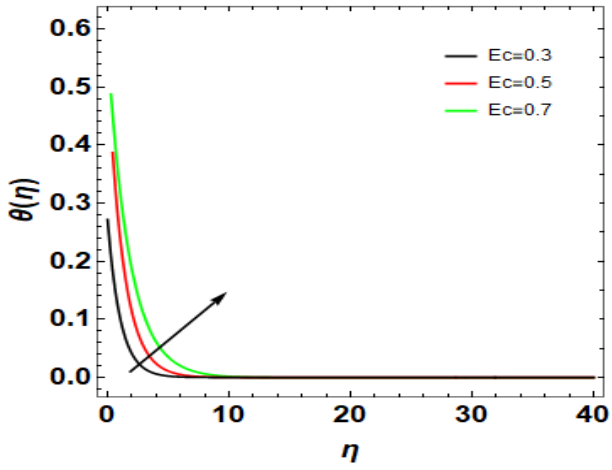

Fig. 10. Effect of Eckert Number *(Ec)* on Temperature distribution

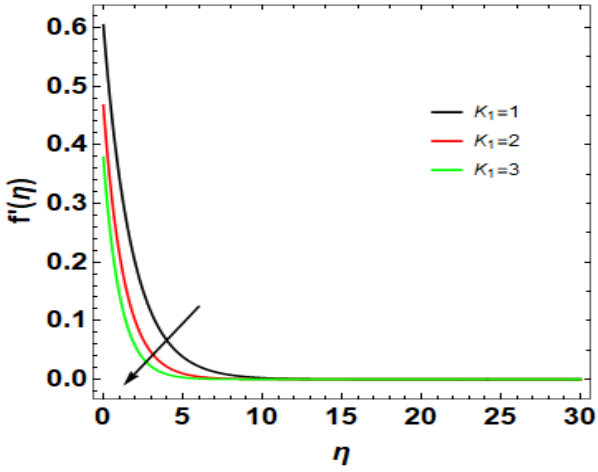

Fig. 11. Effect of Porosity Parameter (k_1) on velocity distribution

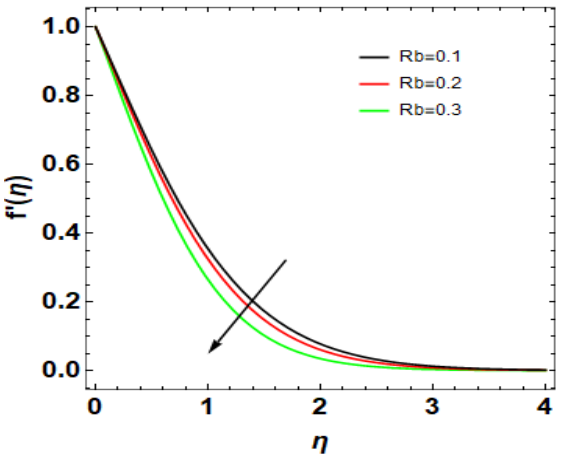

Fig. 12. Effect of Inertial constraint (k_2) on Velocity distribution

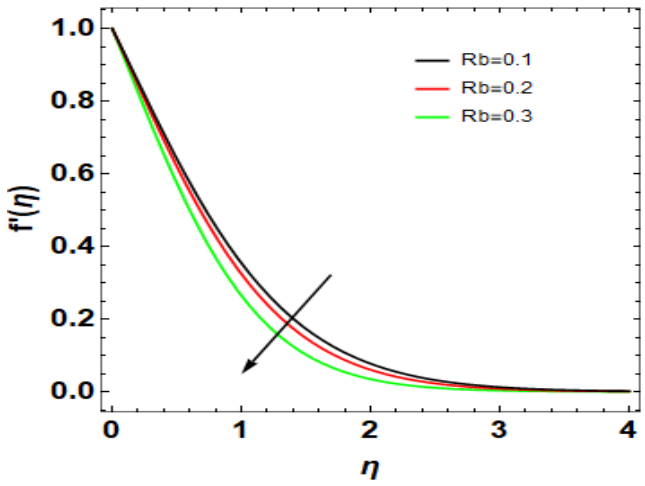

Fig. 13. Effect of Bioconvection Rayleigh *(Rb)* on Velocity distribution

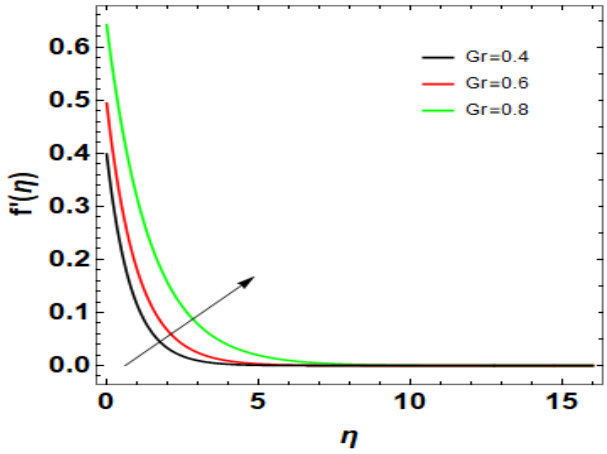

Fig. 14. Effect of Grashof number *(Gr)* on Velocity distribution

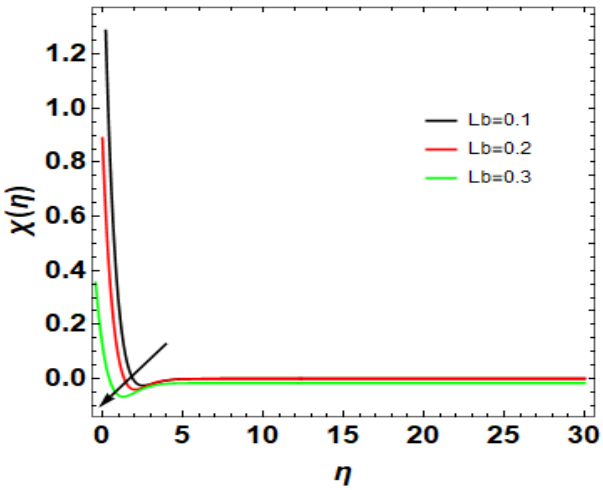

Fig. 15. Effect of Bioconvection Lewis numbers *(Lb)* on microorganism distribution

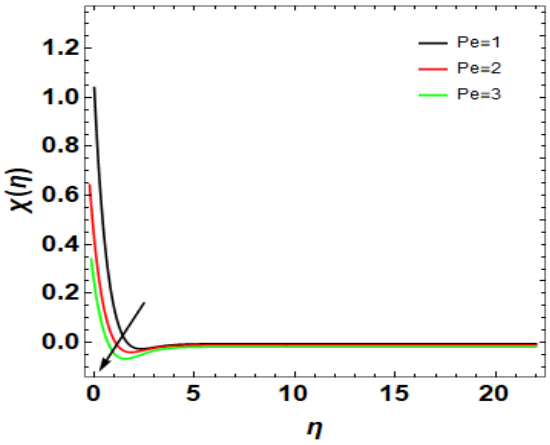

Fig. 16. Effect of Péclet numbers *(Pe)* on motile microorganism distribution

5 Conclusion

The flow, thermal properties, nanoparticle concentration, and motile microorganisms of bioconvective Darcy Forchhemier nanofluid flow across a vertical permeable plate incorporated with chemical reaction parameters and activation energy were investigated in this study. The thermophysical characteristics of gyrostatic microorganisms conducting flow with energy transition were analyzed numerically using CCM with the help of MATHEMATICA software. The findings were analyzed in the form of graphs and tables. The following is a list of some key factors that were discovered in this research:

- The chemical reaction, Thermophoresis and Brownian motion parameter reduces the mass concentration, while large values of activation energy have the opposite effect
- The mounting values of Péclet numbers (Pe) and bioconvection Lewis numbers reduce the Motile microorganism profile.
- Fluid velocity can be enhanced via an increase in buoyancy ratio, porosity constraint, inertial parameter, and Hartmann number.
- The Hartmann number, Eckert number Ec, heat generation elevate the temperature profile.
- The Present study is applicable for the generation renewable energy and building thermal insulation.

Competing Interests

Authors have declared that no competing interests exist.

References

[1] Maxwell JC. Electricity and Magnetism. Clarendon Press, Oxford, UK; 1873.

[2] Yu W, Choi SUS. The role of interfacial layers in the enhanced thermal conductivity of Nanofluids: A Renovated Maxwell Model. Journal of Nanoparticle Research. 2003;5:167–171.

[3] Yu SM. Effect of Nanoparticles on Critical Heat Flux of water in Pool Boiling Heat Transfer. Applied Physics Letters. 2003;83:3374-3376.

[4] Sreelakshmy KR, Aswathy S Nair, Vidhya KM, Saranya TR, Sreeja C Nair. Overview of Recent Nanofluid Research. International Research Journal Pharm. 2014;5(4):1-5.
DOI: 10,7897/2230 – 8407, 050451

[5] Maatoug S, Babu KH, Deepthi VVL, Ghachem K, Raghunath K, Ganteda C, Khan SU. Variable chemical species and thermo-diffusion Darcy–Forchheimer squeezed flow of Jeffrey nanofluid in horizontal channel with viscous dissipation effects. Journal of the Indian Chemical Society. 2023;100(1):100831.

[6] Gaffar SA, Prasad VR, Beg OA. Numerical study of flow and heat transfer of non-Newtonian tangent hyperbolic fluid from a sphere with Biot number effects, Alex. Eng. J. 2015;54:829–841.

[7] Ali A, Asghar S. Analytic solution for oscillatory flow in a channel for Jeffrey fluid, J. Aero. Eng. 2012;27:644–651.

[8] Sharma BD, Yadav PK, Filippov AA. Jeffrey-fluid model of blood flow in tubes with stenosis. Colloid J. 2017;79:849–856.

[9] Seddeek MA. Influence of viscous dissipation and thermophoresis on Darcy Forchheimer mixed convection in a fluid saturated porous media, J. Colloid Interface Sci. 2006;293:137–142.

[10] Kuznetsov AV. The onset of nanofluid bioconvection in a suspension containing both nanoparticles and gyrotactic microorganisms. International Communications in Heat and Mass Transfer. 2010;37(10):1421-1425.

[11] Kuznetsov AV. Nanofluid bioconvection in water-based suspensions containing nanoparticles and oxytactic microorganisms: Oscillatory instability. Nanoscale Research Letters. 2011;6:1-13.

[12] Khan M, Salahuddin T, Malik MY, Mallawi FO. Change in viscosity of Williamson nanofluid flow due to thermal and solutal stratification. International Journal of Heat and Mass Transfer. 2018;941-948.
DOI: 10.1016/j.ijheatmasstransfer.2018.05.074

[13] Kazi SN, Hussein T. An experimental and numerical investigation of heat and mass transfer enhancement for graphic nanoplatelets nanofluids in turbulent flow conditions. Journal of Heat and Mass Transfer. 2015;41-51.

[14] Tzeng SC, Lim CW, Huang KD. Heat Transfer Enhancement of Nanofluids in Rotary Blade Coupling of Four-Wheel-Drive Vehicles. Acta Mechanica. 2005;179:11-23.

[15] Vassallo, Peter, Kumar Ranganathan, D'Amico Stephen. Pool boiling heat transfer experiments in Silica-Water NanoFluids. International Journal of Heat and Mass Transfer. 2004;47:407-411.

[16] Sabet FA. Nanofluid-based sensors and their applications in detection of chemical and biological species: A review. Microchimica Acta. 2018;185(3):213-220.

[17] Farooq U, Tahir M, Waqas H, Muhammad T, Alshehri A, Imran M. Investigation of 3D flow of magnetized hybrid nanofluid with heat source/sink over a stretching sheet, Scientific Reports. 2022;12:12254.

[18] Gandhi R, Sharma B. Combined effects of Joule heating and non-uniform heat source/sink on unsteady MHD mixed convective flow over a vertical stretching surface embedded in a Darcy-Forchheimer porous medium. Propulsion and Power Research. 2022;11(2):276-292.

[19] Gautam AK, Rajput S, Bhattacharyya K, Pandey AK, Chamkha AJ, Begum M. Comparative study of two non-newtonian fluids with bioconvective induced MHDflow in presence of multiple slips, heat source/sink and nonlinear thermal radiation. Chemical Engineering Journal Advanves. 2022;12:100365.

[20] Jawad M, Mebarek-Oudina F, Vaidya H, Prashar P. Influence of bioconvection and thermal radiation on MHD Williamson non casson fluid flow with the swimming of gyrotactic microorganisms due to porous stretching sheet. J. Nanofluids. 2022;11(4):500-509.

[21] Asogwa KK, Goud BS, Reddy YD, Ibe AA. Suction effect on the dynamics of MHD casson nanofluid over an induced stagnation point flow of stretchable electromagnetic plate with radiation and chemical reaction, Results in Engineering. 2022;15:100-518.

[22] Eswaramoorthi S, Thamaraiselvi S, Loganathan K. Exploration of darcy-forchheimer flows of non-newtonian casson and Williamson conveying tiny particles experiencing binary chemical reaction and thermal radiation: comparative analysis. Maths. Comput. Appl. 2022;27:52.

[23] Jawad M, Saeed A, Gul T, Bariq A. MHD Darcy-Forchheimer flow of Casson nanofluid due to a rotating disk with thermal radiation and Arrhenius activation energy. Journal of Physics Communications. 2021;5(2):025008.

[24] Nadab H, Amoo SA, Olopade IA. Heat and mass transfer analysis of magnetohydrodynamic (MHD) thermosolutal nanofluid flow over vertical and inclined porous media. International Journal of Mathematical Analysis and Modelling. 2023;6(2).

[25] Yusuf TA, Mabood F, Prasannakumara BC, Sarris IE. Magneto-Bioconvection Flow of Williamson Nanofluid over an Inclined Plate with Gyrotactic Microorganisms and Entropy Generation . Fluids. 2021;6(3):109-120.
DOI: 10.3390/fluids603010

[26] Abdel MS, Mahantesh M, Nandeppanava K, Sharanagouda B, Malipatil A. Heat transfer in a second grade fluid through a porous medium from a permeable stretching sheet with non-uniform heat source/sink. International Journal of Heat and Mass Transfer. 2010;53(9-10):205-217.

[27] Srinivas S, Kalyan Kumar C, Badeti S, Reddy AS. MHD Flow of Casson Nanofluid over an inclined porous stretching surface. In Recent Advances in Applied Mathematics and Applications to the Dynamics of Fluid Flows: 5th International Conference on Applications of Fluid Dynamics (ICAFD) 2020 (pp. 155-165). Singapore: Springer Nature Singapore; 2022, October.

[28] Srinivas S, Challa KK, Badeti S, Kumar PB. Pulsatile powell-eyring nanofluid flow in a channel with inclined magnetic field and chemical reaction. Engineering Transactions. 2023;71(4):519-535.

[29] Srinivas S, Kumar CK, Reddy AS. Dufour and Soret effects on pulsatile hydromagnetic flow of Casson fluid in a vertical non-Darcian porous space. Nonlinear Analysis: Modelling and Control. 2022;27(4):669-683.

[30] Algehyne EA, Areshi M, Saeed A, Bilal M, Kumam W, Kumam P. Numerical simulation of bioconvective Darcy Forchhemier nanofluid flow with energy transition over a permeable vertical plate. Scientific Reports. 2022;12(1):3228.

[31] Makinde OD, Aziz A. Boundary layer flow of a nanofluid past a stretching sheet with a convective boundary condition. International Journal of Thermal Sciences. 2011;50:1326-1332.

[32] Khan W, Pop I. Boundary-layer flow of a nanofluid past a stretching sheet. International Journal of Heat. 2010;53:2477-2483.

[33] Abolbashari MH, Freidoonimehr N, Nazari F, Rashidi MM. Analytical modeling of entropy generation for Casson nano-fluid flow induced by a stretching surface. J Advanced Powder Technology. 2015;26:542-552.

Peer-review history:
The peer review history for this paper can be accessed here (Please copy paste the total link in your browser address bar)
https://prh.globalpresshub.com/review-history/1451